ELSEVIER

Biophysical Chemistry 71 (1998) 35–50

Biophysical Chemistry

Dynamic properties of individual water molecules in a hydrophobic pore lined with acyl chains: a molecular dynamics study

Zhi Qi, Masahiro Sokabe *

Department of Physiology, Nagoya University School of Medicine, 65 Tsurumai, Nagoya 466, Japan

Received 20 August 1997; revised 29 October 1997; accepted 20 November 1997

Abstract

Recently, a certain class of synthetic molecules has been shown to form ion channels, the pore of which is lined with hydrophobic acyl chains [M. Sokabe, in: F. Oosawa, H. Hayashi, T. Yoshioka (Eds.), Transmembrane Signaling and Sensation, JSSP/VNU Science Press BV, Tokyo, 1984, p. 119; F. Hayashi, M. Sokabe, M. Takagi, K. Hayashi, U. Kishimoto, Biochim. Biophys. Acta, 510 (1978) 305; M.J. Pregel, L. Jullien, J. Canceill, L. Lacombe, J.M. Lehn, J. Chem. Soc. Perkin Trans., 2 (1995) 417; Y. Tanaka, Y. Kobuke, M. Sokabe, Angew. Chem. Int. Ed. Engl., 34 (1995) 693; M. Sokabe, Z. Qi, K. Donowaki, H. Ishida, K. Okubo, Biophys. J., 70 (1996) A201; H. Ishida, K. Donowaki, Y. Inoue, Z. Qi, M. Sokabe, Chem. Lett. (1997) p. 953]. As an initial step towards understanding the physical mechanisms of ion permeation across such a hydrophobic pore, systematic molecular dynamics simulations were performed to investigate dynamic and energetic properties of water molecules inside the pore using a dimer of alanine-*N*′-acylated cyclic peptide as a channel model. Dynamic energy profiles for water molecules indicated that the energy barrier at the middle region of the pore is approximately 2–3 kcal/mol higher than that in the cap water region which was defined as a vicinity region of the channel entrance. Energetics analyses demonstrated that the mutual interactions among intrapore water molecules are the major factor to give favorable interaction (negative energy contribution) for themselves. The pore, despite being lined with acyl chains, has a favorable van der Waals interaction with intrapore water molecules. These results may help to explain why water-filled channels can be formed by the hydrophobic helices in natural channels. © 1998 Elsevier Science B.V.

Keywords: Water-filled channel; Hydrophobic pore; Nonbonded interaction; Molecular dynamics (MD); Dynamic energy fluctuation

1. Introduction

It was indicated decades ago that an aqueous pore must span the membrane to facilitate the transport of ions through the membrane [1]. It has been believed that the pore interior should be lined with charged or polar groups to provide environment which stabilizes water and ions when they repeatedly alternate their solvation structure during internal diffusion across the pore [2]. Such a conventional idea, however, has been challenged by recent findings that a certain class of lipid molecules and a kind of de novo synthesized molecules composed mainly of poly

* Corresponding author. Tel.: +81-52-744-2051; fax: +81-52-744-2057; e-mail: e43429a@nucc.cc.nagoya-u.ac.jp

PII S0301-4622(97)00134-8

nonpeptide chains could form ionic channels, the pore of which is supposed to be lined with relatively hydrophobic chains [3–8]. A pore filled with water is a prerequisite for the permeation of the ion, so an issue of primary importance is to know the physical properties of intrapore water molecules and the interactions with their surrounding environment, the channel, the bulk water and the membrane.

The properties of water in a hydrophobic pore have been intensively studied recently with the technique of molecular dynamics simulations. Creating channel-like hydrophobic cavities to confine water molecules, Sansom et al. [9] have performed molecular dynamics simulations to compare the structure and dynamics of water molecules in the cavities with those in the bulk water. Constructing model channels which were composed of bundle of hydrophobic peptide helices, Breed et al. [10] have run molecular dynamics simulations to analyze the mobility and dipole orientations of the intrapore water molecules. Those studies found some common features of intrapore water, namely immobilization of water molecules within the cavities or pores; preferential orientation of intrapore water dipoles along the channel axis. The question of how water molecules could stably occupy a pore without any polar pore-lining side chains, however, still remains to be answered [10], due to lack of data on the energetics, especially dynamic energetics, of intrapore water. One way to solve this problem is to study the properties of water in a pure hydrophobic pore with minimal structure that can mimic channel-like properties. By taking this approach, we may extract basic features of intrapore water, which would eventually help to obtain insights into the behavior of the water in natural channels.

Here we consider the channel formed by a dimer of a synthetic tetrameric molecule of alanine-*N′*-acylated diaminobenzoic acid, cyclo((Ala-Daba(C16)-)4 [8], AC164 for abbreviation. A dimer of AC164 molecule was designed to form a channel with a pore lined with pure hydrophobic acyl chains (derived from palmitic acid). Placed in asolectin bilayer membranes, the AC164 channel could mimic typical single channel behaviors and makes a pore with diameter around 6 Å [11]. In the present study, two different force fields (CVFF and AMBER) were used to perform MD simulations on the water-filled channel system of AC164 in order to extract force field-independent features. Results were analyzed: (1) through the energy decomposition technique to answer why the water molecules could stably occupy a pore lined with pure hydrophobic acyl chains; (2) according to the trajectories of individual water molecules to know their dynamic properties; (3) in terms of dynamic nonbonded interactions between individual intrapore water molecules and the rest of the system to elucidate their energy fluctuation properties. The dynamic energy profiles and trajectories that are basically common to different force field simulations were obtained. Similar conclusions drawn from two different force fields may provide a strong basis for the present study.

2. Materials and methods

2.1. General

All results were obtained using programs from Biosym/MSI of San Diego. Molecules were built with the *Builder* program with partial charges from CVFF force field. Conformational search was carried out using CVFF force field; Other minimizing and dynamics calculations were done with the *Discover®* program, using both AMBER and CVFF force fields; Graphical displays were printed out from the *Insight® II* molecular modeling system. Force field parameters for nonbonded interactions used in the MD simulations were listed in Tables 1 and 2.

2.2. Model of the channel system

2.2.1. Conformational search of the monomer via simulated annealing and restrained molecular dynamics (SA/MD)

SA/MD modeling method has been proved to be a powerful tool in searching conformations of various molecules [12,13], it enables us to explore a wider range of conformational space. Using SA/MD, we carried out conformational search on the monomer of AC164 molecule in three stages. In stage I, a primitive structure was built with the Builder module of *Insight® II* (a graphical platform software) according to its one dimensional sequence [8] with

Table 1
Nonbonded atom type definitions in CVFF force field

Element	Potential type	A	B
H	h Hydrogen bonded to C	7108.466	32.87076
H	hn Hydrogen bonded to N	0.00000001	0.00000
H	h* Hydrogen in water molecule	0.00000001	0.00000
C	c′ Sp2 carbon in carbonyl (C=O) group	2,968,753.3590	1325.70810
C	cp Sp2 aromatic carbon (partial double bonds)	2,968,753.3590	1325.7081
C	ca General amino acid alpha carbon (Sp3)	1,790,340.7240	528.48190
C	c3 Sp3 carbon in methyl (CH3) group	1,790,340.7240	528.48190
C	c2 Sp3 carbon bonded to 2 H's, 2 heavy atoms	1,790,340.7240	528.48190
N	n Sp2 nitrogen with 1 H, 2 heavy atoms (amide group)	2,266,872.4	123.5570
O	o′ Oxygen in carbonyl (C=O) group	272,894.7846	498.87880
O	o* Oxygen in water molecule	629,358.00000	625.500000

Lennard–Jones potential $E = A_{ij}/r_{ij}^{12} - B_{ij}/r_{ij}^{6}$ (where $A_{ij} = \sqrt{A_i \times A_j}$ $B_{ij} = (B_i \times B_j)$).

exactly four-fold rotational symmetric configuration. Consequently, a cylindrical cavity with diameter of approximately 9 Å was formed from completely parallel acyl chains, the carbon and hydrogen atoms of which were superimposed upon each other. A modified flatbottomed function (see *Insight® II User Guide 2-23*, San Diego: Biosym/MSI, 1995),

$$E = 0 \quad d < d1 \tag{2.1a}$$

$$E = \text{scale} \times k \times (d - d1)^2 \quad d \geq d1, \tag{2.1b}$$

was used to restrain the cavity small enough, where scale is the restraint scale factor and k is force constant. In this expression, d is the current distance between two restrained atoms, each of which comes from the corresponding carbon atom of adjacent- or cross-chain. And $d1$ was assigned 3.5 and 4.9 Å for adjacent- and cross-chain carbon atoms, respectively, to make the diameter of the cavity approach zero. The purpose of doing so was to find a starting conformation for stage II, in which the cavity will simply expand in the conformational search process. No restraint was imposed on the atoms of the ring at stage I. The scale factors of all the interactions (bond or nonbonded) were set as small values at first and were gradually increased during minimization. Once the scale factor for these terms reached 1 and the maximal derivative of the minimization was less than 0.01 kcal/mol, a 100 ps MD run of 1 fs time step (stage II) were employed at the temperature of 1000 K and the conformations were saved every 0.1 ps for conformational analyses. Due to its inherent fourfold rotational symmetry of the channel struc-

Table 2
Nonbonded atom type definitions in AMBER force field

Element	Potential type	R_i^*	EPS_i
H	HC explicit hydrogen attached to carbon	3.0800	0.01000
H	H amide hydrogen	2.0000	0.02000
H	HW hydrogen in water	0.0001	0.00001
C	CA sp2 aromatic carbon in 6-membered ring with 1 substituent	3.7000	0.12000
C	C sp2 carbonyl carbon	3.7000	0.12000
C	CT sp3 carbon with 4 explicit substituents	3.6000	0.06000
N	N sp2 nitrogen in amide group	3.5000	0.16000
O	O carbonyl oxygen	3.2000	0.20000
O	OW water oxygen	3.5360	0.15200

Lennard–Jones potential $E = \text{EPS}_{ij} \times \{(R_{ij}^*/R_{ij})^{12} - 2(R_{ij}^*/R_{ij})^6\}$ where $\text{EPS}_{ij} = \sqrt{\text{EPS}_i \times \text{EPS}_j}$ $R_{ij}^* = (R_i^* + R_j^*)/2$.

ture, which was confirmed by the mass spectroscopy and NMR spectra data [8], a relatively large harmonic potential

$$E = \text{scale} \times k \times (d - d_0)^2 \qquad (2.2)$$

was applied to restrain the above paired atoms in stage I as well as the same kind of paired heavy atoms (oxygen, nitrogen and carbon) from the ring to keep the symmetric conformation of the AC164 monomer at 1000 K, where d_0 is the average distance of corresponding paired heavy atoms initially obtained from the end of stage I and updated after every 100fs during stage II. Full conformations generated at 1000 K were grouped into five families by creating families of structures that had mutual root mean square deviations (RMSDs) less than a threshold value of 1.6 Å. In stage III, the average conformation of each family was cooled from 1000 K to 300 K at the rate of 7 K per 100 steps. During cooling, restraint constants were reduced at each temperature. After reaching 300 K, minimization was carried out on each conformation with a small restrain to keep the symmetry of the monomer. Some of those preliminary results have appeared in an abstract form [14].

2.2.2. Constructing the channel system

Experimental results showed that the conductance of the designed channels of AC164 series with different ring size and different acyl chain length did not have significantly different values, implying that the conformation of the peptide ring and the acyl chain length should not play an important role in the process of ion permeation [7]. On the other hand, our purpose right now is to study the dynamic properties of water molecules inside the pore lined with pure hydrophobic acyl chains. Therefore, the conformation, the diameter of which was approximately the same as that of methylammonium ion (Fig. 1a), the largest permeant ion of the AC164 channel, was simply selected from cooled conformations. A channel was constructed by connecting two monomers together with staggered-trans configuration with a length of about 40 Å (Fig. 1b and c), approximately the thickness of the lipid bilayer membrane [15] and with a diameter of about 6 Å, approximately the diameter of a methylammonium ion. The primary solvation of the channel was provided by building 27 water molecules into the pore which are called intrapore water in our simulations, 13 on each side of the monomer and one in the center of the pore. 'Bulk water' is approximated by hemispherical regions (cap regions) of a pre-equilibrated water layer with the radius of 20 Å at each end of the channel. Similar to described elsewhere [2,16], the channel and its intrapore water were embedded in 640 pre-equilibrated $-CH_2-$ particles (Lennard–Jones particles with no charge or polarizability), which were constructed according to the density of hydrocarbon core of lipid bilayers obtained from MD simulation of dipalmitoylphosphatidylcholine [15], to produce a hydrocarbon-like environment of the lipid bilayer membrane (model membrane) and to prevent water molecules from reaching the lateral side of the pore. For easy manipulation of the calculation, the 'bulk water' was divided into 3 layers of solvent with 126 molecules in inner layer, 297 in middle layer and 628 in outer layer. The model membrane was also divided into three layers with 132, 138 and 370 $-CH_2-$ residues in inner, middle and outer layer, respectively (Fig. 1d). A coordinate system was constructed, in which the mass center of the dimer was placed at the origin and the channel axis, defined as the line going through the mass center of each monomer, was oriented along the x axis (Fig. 1c).

Fig. 1. Description of the channel system. Color coding is as follows unless otherwise noted: oxygen atoms are red; hydrogen atoms are white; carbon atoms are green; and nitrogen atoms are blue. (a) Methylammonium ion with its biggest and smallest section area. (b) CPK model of the AC164 channel viewed down from x-axis. (c) CPK model of the channel with its coordinate system. (d) Channel system with its components. Acyl chains of the pore are represented with green ribbons. The peptide ring of the channel is shown by the stick. Twenty-seven intrapore water molecules, which were used to make primary solvation of the channel, are shown by CPK model with some of them deleted to show the peptide ring. Inner layer of 'bulk' water molecules and $-CH_2-$ particles are represented with cyan and yellow colored balls. Other layers of water molecules and $-CH_2-$ particles are shown by sticks. The junction between the peptide ring and the acyl chains is indicated by arrows.

2.3. MD simulation details

To attain common conclusions, the consistent-valence force field (CVFF) [17], which has been well tested and characterized in the *Discover* program and the AMBER force field [18], which has been widely used not only for proteins and DNA, but also for many other classes of molecules such as poly-

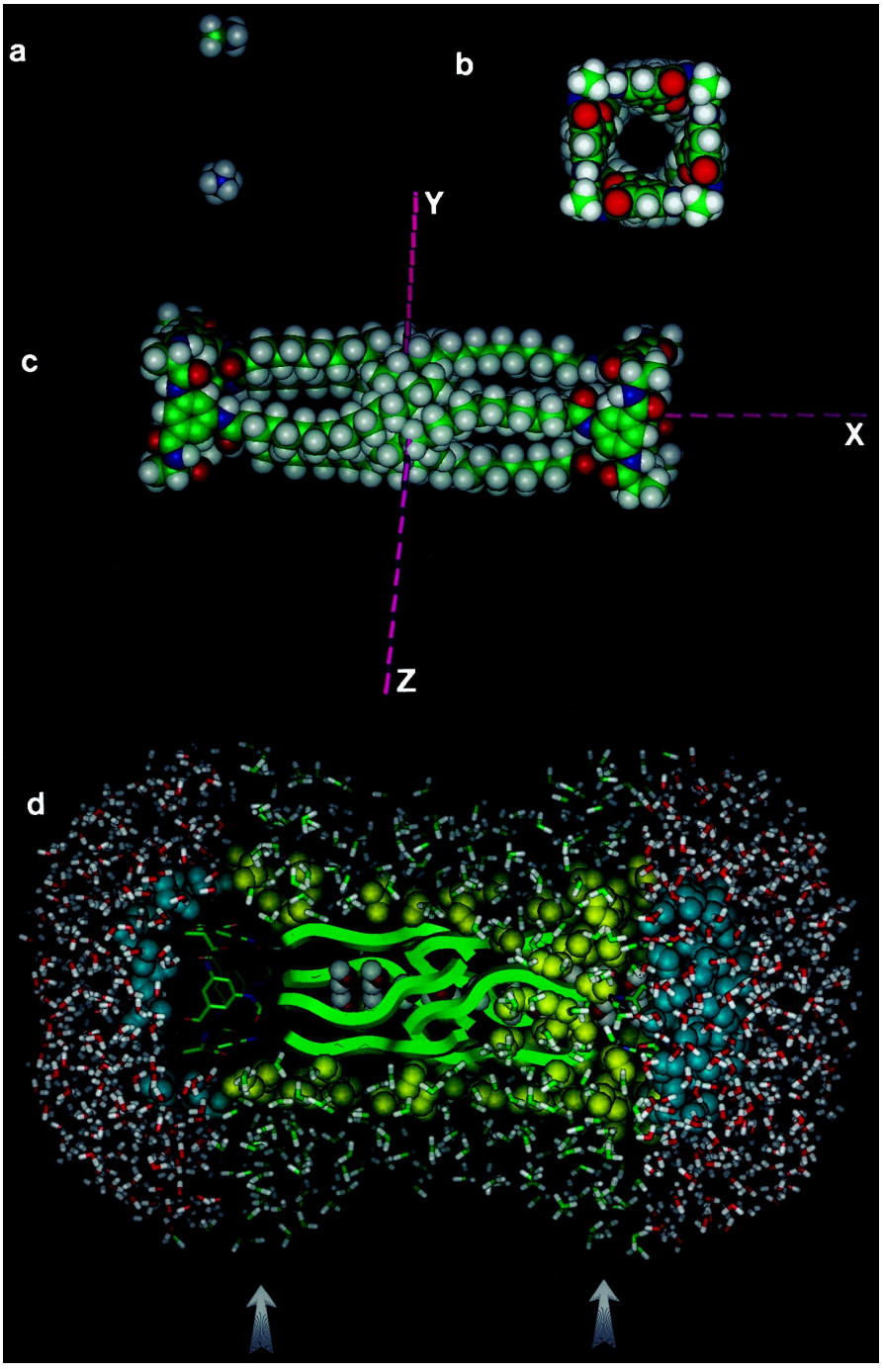

mers and small molecules, were applied on the systematic runs of our channel system under exactly the same conditions to be described below.

First, the entire system was subjected to a four-stage energy minimization to refine the configuration of the whole system: (a) Steepest descents minimization method was employed, followed by the conjugate gradient method (Polak–Ribiere) until maximum derivative was less than 0.5 kcal/mol. The purpose of this stage is to find suitable positions for water molecules and $-CH_2-$ particles in outer layers relative to those in the middle and inner layers. So the atoms of the pore and intrapore water molecules were fixed, while all the solvent particles (water and $-CH_2-$ particles) were set free to move. (b) The water molecule at the center of the pore, outer layers of water molecules and $-CH_2-$ particles were fixed. The intrapore water except the one at the center was set free. The atoms of other parts were strongly tethered around their original positions. Then 10 loops of minimization were run while the force constant of tether was gradually reduced to a small value. By doing this, the middle layer of water molecules and $-CH_2-$ particles approached their suitable configurations. (c) To find the optimal configuration in interface between 'bulk' and intrapore water, the following strategies were adopted: the outer and middle layers of water molecules and $-CH_2-$ particles as well as the water molecule at the center of the pore were fixed; the pore was tethered; the intrapore water except the one at the center, inner layers of water molecules and $-CH_2-$ particles were set free. The minimization was carried out till the maximum derivative was less than 0.1 kcal/mol; The aim of (d) is to get suitable condition for the MD run. The so-called extended wall region boundary condition [19] was employed as a strategy of compromise, trading accuracy against saving computer time. The extended wall region was achieved by fixing outer and middle layers of water molecules and $-CH_2-$ particles, within which a buffer region between unfixed part of the system and the unrealistic vacuum surrounding was formed. The pore was weakly tethered in order to study the permeation property of water through the open channel. The inner layer of $-CH_2-$ particles was also weakly tethered to prevent them from penetrating into the channel too deep. From this step, all intrapore water molecules, including the one at the center of the pore and inner layer of water molecules were set free to move in order to approach a realistic environment for intrapore water molecules.

Second, after the maximal derivative of the final minimization was less than 0.01 kcal/mol, two-stage MD simulations at a time step of 0.5 fs were performed at the temperature of 298 ± 10 K with CVFF or AMBER force field, respectively. The equilibration stage was run for 10 ps. Random initial velocities were generated at 298 K from Boltzmann distribution. The data collecting stage, the thermodynamic quantities of which are shown in Table 3, was run for 200 ps with coordinates of all the atoms saved every 0.1 ps (corresponding to 2000 conformations) for later analyses. These 2000 conformations were replayed later to calculate temporal and spatial variations of inter- and intra-nonbonded interactions of channel water. Verlet velocity integrator was applied in all calculations. Group based nonbonded interactions between distant atoms were smoothly turned off using a switching function and a cutoff distance of 9.5 Å along with the spline width of 1 Å and the buffer width of 0.5 Å. Canonical ensemble was used as a statistical ensemble. Nosé dynamics [20], which is a relatively new method for performing constant-temperature and true canonical ensemble dynamics, was employed during simulations.

The nonbonded interaction energies between the intrapore water as a whole and other components of the system, as well as the nonbonded interaction energies between each intrapore water molecule and

Table 3
Thermodynamic quantities in data collecting stage of the MD run

Force field	Total energy[a]	Kinetic energy[a]	Potential energy[a]	Temperature (K)
AMBER	-424.3 ± 36.8	1248.6 ± 26.3	-1672.9 ± 30.3	290.8 ± 6.3
CVFF	-187.3 ± 36.6	1243.0 ± 26.4	-1430.3 ± 26.6	291.0 ± 6.2

[a] The unit of energy is kcal/mol.

all of the rest of the atoms including other intrapore water molecules, were calculated by the Energy Analysis command of the Insight program. This command can be used to output either the total nonbonded energies or the interaction energies between the molecular objects, which can be any collection of atoms, residues, monomers and molecules. The energy of a molecular object can be broken down into internal (intra) and external (inter) portions. If we concentrate on the nonbonded interactions (van der Waals and electrostatic terms), the internal energy is the sum of the nonbonded interactions between the atoms in the molecular object. The interaction energy between any two objects is the sum of the nonbonded interactions between all pairs of atoms where one atom is in the first object and the other atom is in the second object. The external energy of an object is a half of the sum of the interaction energies between itself and the rest of the system. The factor of $1/2$ apportions the interaction energy equally between the two objects, accounting for the fact that the interaction between I and J is the same as the interaction between J and I. Given these definitions, if we break the system down into some number of components, the sum of the internal and external energies of the components is the same as the total nonbonded energy of the entire system.

3. Results and discussions

3.1. Energetics of intrapore water

To find a clue to understand why the water molecules could stably occupy a channel with pure hydrophobic lining, it is useful to partition total interaction energy of intrapore water molecules ($E_{\mathrm{Tol-W}}$) into interactions that come from themselves and other components of the system. These interactions involve the intrapore water molecules among themselves, $E_{\mathrm{W-W}}$, the intrapore water molecules with the channel, $E_{\mathrm{W-Ch}}$, the intrapore water molecules with the inner layer of cap water molecules, $E_{\mathrm{W-Icap}}$ and the intrapore water molecules with the rest of the system (the middle and outer layer of cap water molecules as well as the model membrane), $E_{\mathrm{W-Other}}$. With these conventions, the interaction energy of the intrapore water could be written as:

$$E_{\mathrm{Tol-W}} = E^{\mathrm{Coul}}_{\mathrm{W-W}} + E^{\mathrm{Vdw}}_{\mathrm{W-W}} + E^{\mathrm{Coul}}_{\mathrm{W-Ch}} + E^{\mathrm{Vdw}}_{\mathrm{W-Ch}} + E^{\mathrm{Coul}}_{\mathrm{W-Icap}} + E^{\mathrm{Vdw}}_{\mathrm{W-Icap}} + E_{\mathrm{W-Other}} \qquad (3.1)$$

where Coul and Vdw are for coulombic and van der Waals interactions, respectively. Fig. 2 shows the results on these interactions, with thick lines for $E_{\mathrm{W-W}}$, medium lines for $E_{\mathrm{W-Icap}}$ and thin lines for $E_{\mathrm{W-Ch}}$. As other layers of cap water and $-CH_2-$ particles have little effect on the energy level of intrapore water, their energy contributions, $E_{\mathrm{W-Other}}$, are not shown in the figure. By comparing thick lines with medium and thin lines in Fig. 2a and c, or Fig. 2d and f, we found that the main factor to give favorable interactions to the intrapore water molecules arises from their own coulombic interactions, $E^{\mathrm{Coul}}_{\mathrm{W-W}}$. In contrast, we found that the van der Waals interactions among themselves, $E^{\mathrm{Vdw}}_{\mathrm{W-W}}$, give unfavorable interactions to the intrapore water molecules (see thick lines in Fig. 2b and e). A surprising result is that the van der Waals interaction with the channel, $E^{\mathrm{Vdw}}_{\mathrm{W-Ch}}$, gives negative energy contribution to the intrapore water molecules (thin lines in Fig. 2b and e), in spite of the channel being lined with acyl chains. This favorable interaction might be caused by the flexibility of the acyl chains, since the value of this interaction energy was relatively more positive when the acyl chains were fixed (data not shown). Similarly it has been shown that the computed total interaction energy of the gramicidin A channel–Na^+–water system is lower with flexible ethanolamine tails than that with fixed tails [21]. This might mean that the complex of the channel and its intrapore water molecules could continuously 'find' a configuration in which the distance between the intrapore water molecule and its closest atom(s) from the channel is in favor of their attractive dispersion interaction, due to the flexibility of the acyl chains. Very recently it has been recognized that the C–H $\cdots$ O contact can exhibit typical features of hydrogen bond in biological macromolecules and thus contributes to the overall stabilization of the macromolecules and their complexes (for review, see Ref.[22]). Taking this fact into account, we may speculate that an oxygen of an intrapore water molecule with its lone-pair orbital preferentially ap-

proaches a hydrogen to form a C–H · · · O type hydrogen bond temporarily. Therefore, the sum of such interactions between the channel and the intrapore water molecules may contribute to the stability of the channel–water complex.

We are not able to determine when and which water molecule will enter into the pore region from the cap region (see Fig. 6d or h for definition of the regions) or diffuse away from the pore region to the cap region, so we defined the 27 primary solvation

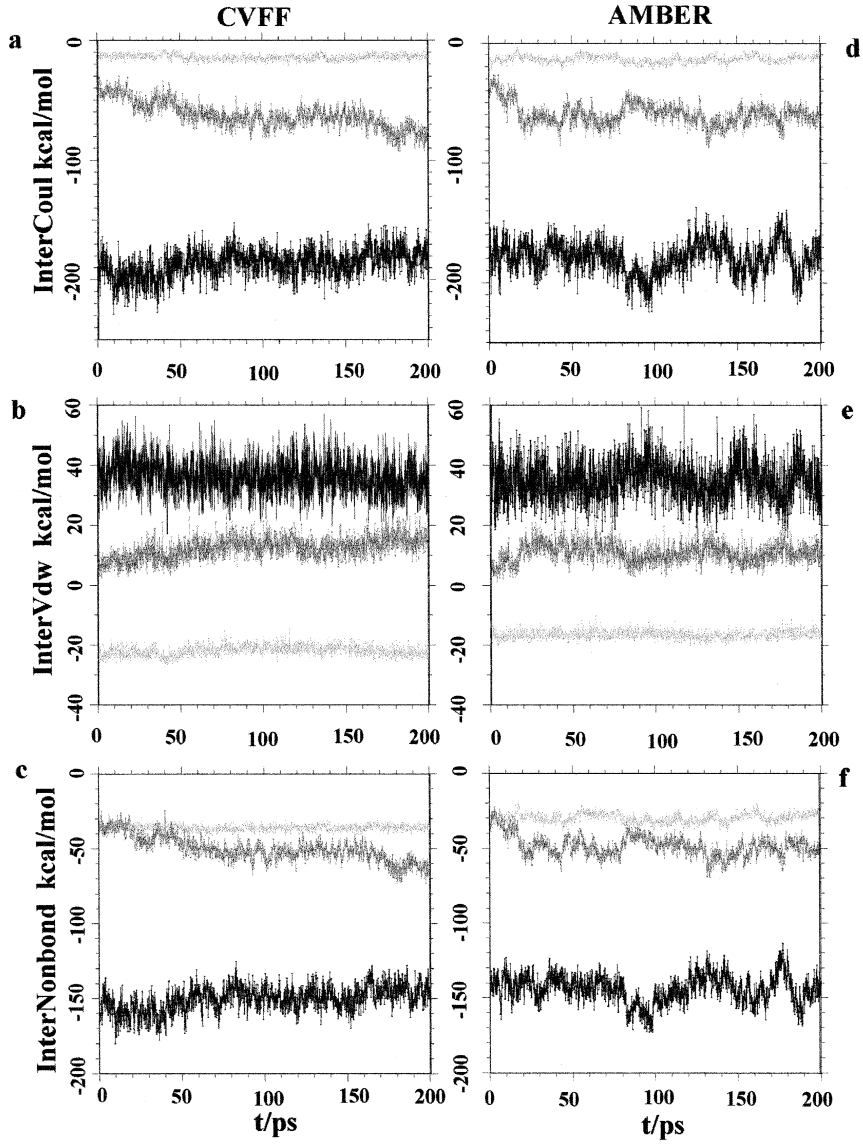

Fig. 2. The nonbonded interaction energy between 27 intrapore water molecules and other components of the system and among themselves as a function of time calculated from CVFF or AMBER force fields: (a and d), Coulombic interactions; (b and e), van der Waals interactions; (c and f), total nonbonded interaction. Thick lines represent the mutual interaction (intra-) among intrapore water molecules, E_{W-W}. Medium lines represent the interactions between the intrapore water molecules and the inner layer of cap water molecules, E_{W-Icap}. Thin lines represent the interactions between the channel and the intrapore water molecules, E_{W-Ch}.

water molecules of the channel (see Section 2.2.2) as intrapore water molecules in our simulations. A problem of this definition is that the intrapore water molecules are not always the 'true' intrapore water molecules, because some of the intrapore water molecules diffused away from the pore and entered into the cap region of the channel. As a result, instead of keeping constant values, the interaction energies were varied with time. However, the system were in dynamic equilibrium state (see Section 3.4), so the conclusion should be valid. Furthermore, the overall results are consistent with each other. For example, it is the exit of some intrapore water molecules from relatively high energy region (pore region) to relatively low energy region (the cap region) that causes $E^{\mathrm{Coul}}_{\mathrm{W-Icap}}$ and $E^{\mathrm{Tol}}_{\mathrm{W-Icap}}$ gradually going down with time (medium lines in Fig. 2a,c,d and f). These results may help to explain why water-filled ion channels can be formed by hydrophobic helices.

3.2. Trajectories of water molecules

It has been demonstrated in the gramicidin channel that the number of water molecules inside the channel plays an important role in internal diffusion of ions and water [23,24]. A completely different behavior has been observed when the number of water molecules placed inside the channel is different. If less number of water molecules is placed inside the channel, a large gap between water molecules becomes obvious. On the contrary, with more water molecules, the mobility of the water and ions is significantly decreased, i.e., the water structure becomes artificially frozen. As we do not have information on the number of water molecules inside our AC164 channel, an alternative method was employed: the intrapore water and the inner layer of cap water molecules were set free to move so that the number of water molecules would be determined by the system itself. Fig. 3 demonstrated trajectories of 33 water molecules, among which 27 of them were used to make the primary solvation of the channel and six of them were selected from cap water molecules, which could penetrate into the pore during the MD run. To make a clear view, typical trajectories of the water molecules were emphasized with thick lines, others were plotted with thin lines. Because of the flexibility of acyl chains, exchanges of water molecules among intrapore water molecules (shown by the trajectories of 4 and 5 in Fig. 3a or (4), (5) and (6) in Fig. 3b) or between intrapore and cap water molecules (shown by the trajectories of 1, 2, 3 and 7, 8 in Fig. 3a as well as (1), (2), (3) and (7), (8) in Fig. 3b) were observed, the phenomenon which could be observed more clearly on animations of the MD runs.

Fig. 3 also shows that the density of the water molecules depends on their location: water molecules are denser in cap and middle region than at the junction region between acyl chains and the peptide ring of the channel (indicated by larger arrows). This phenomenon is consistent with the structure of the channel. The limited space of the rigid structure of the peptide ring may prohibit two water molecules occupying the junction at the same time. The carbonyl oxygen connected to the diaminobenzoic acid may provide a relatively hydrophilic environment for the water molecule, thus giving an energy well for the water. When a water molecule enters into this well, it would stay there until obtaining enough energy from its surroundings. Therefore, even though water molecules could alternatively occupy the 'binding site', only one can stay there at most of the time (also see discussion in Section 3.3). In the single file region of the gramicidin channel, the entire chain of water molecules was observed to move as a single entity, due to the high degree of correlation among the channel water molecules [25]. Correlated motions of water molecules, i.e., neighboring water molecules move towards the same direction and then change their directions of movement simultaneously, can still be observed in this hydrophobic channel, albeit temporally and limited in a small region. So the correlated motion of water molecules is not an exclusive property of peptide channels.

It is interesting that a small gap was created and then filled with water during simulation with AMBER force field (Fig. 3b). Since gaps, which break the continuous hydrogen-bonded water chains, have also been found in the MD run of the gramicidin-like channels [26], it is possible that the perfect hydrogen-bonded network of water molecules can be broken over a significant time period (ca. 50 ps in Fig. 3b). However, we do not know why a gap was

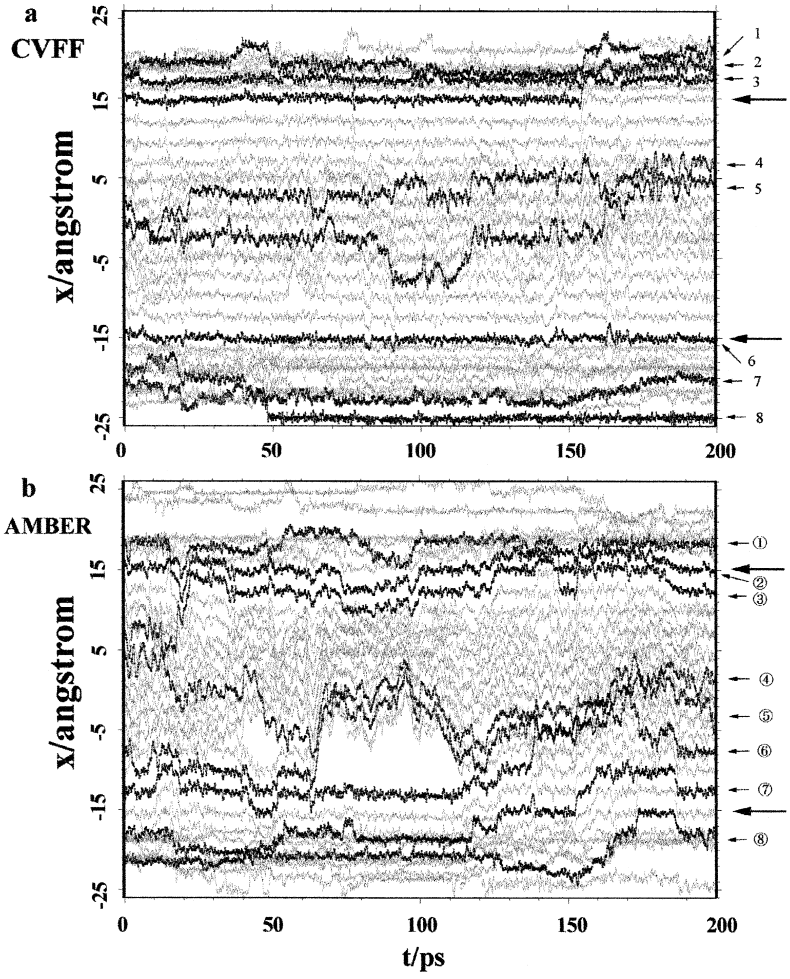

Fig. 3. Plot of trajectories of 33 water molecules, among which 27 of them were used to make the primary solvation of the channel and 6 of them were selected from cap water molecules which could penetrate into the pore during MD runs. Data were calculated by using CVFF force field (a) or AMBER force field (b). Typical trajectories are emphasized by thick black lines in the plot and indicated by small arrows. Other trajectories are plotted with thin lines. Large arrows indicate the position of the junction between peptide ring and acyl chains.

created in the simulation with AMBER force field, but not with CVFF force field. The limited time of the MD run may probably be the reason to cause such difference.

Careful analyses of the trajectory of individual water molecules nicely showed the characteristics of diffusion in different regions of the channel. Fig. 4 illustrates such analyses by zooming in trajectories of water molecules located at left (a and d), middle (b and e) and right (c and f) side of the pore. The displacement fluctuations of the mass center of water molecules along the channel depend on their location. Comparing Fig. 4b with Fig. 4a and c or comparing Fig. 4e with Fig. 4d and f, we found that the water molecules at each end of the channel fluctuate more frequently than the one at the middle part of the channel. This means that the cap water molecules change their direction of movement more frequently than that of the intrapore water molecules do, suggesting that water molecules undergo more collisions with their neighboring particles in the cap region than in the intrapore region. The cap water molecules are surrounded by ‘bulk’ water molecules, which have much more freedom of movement than

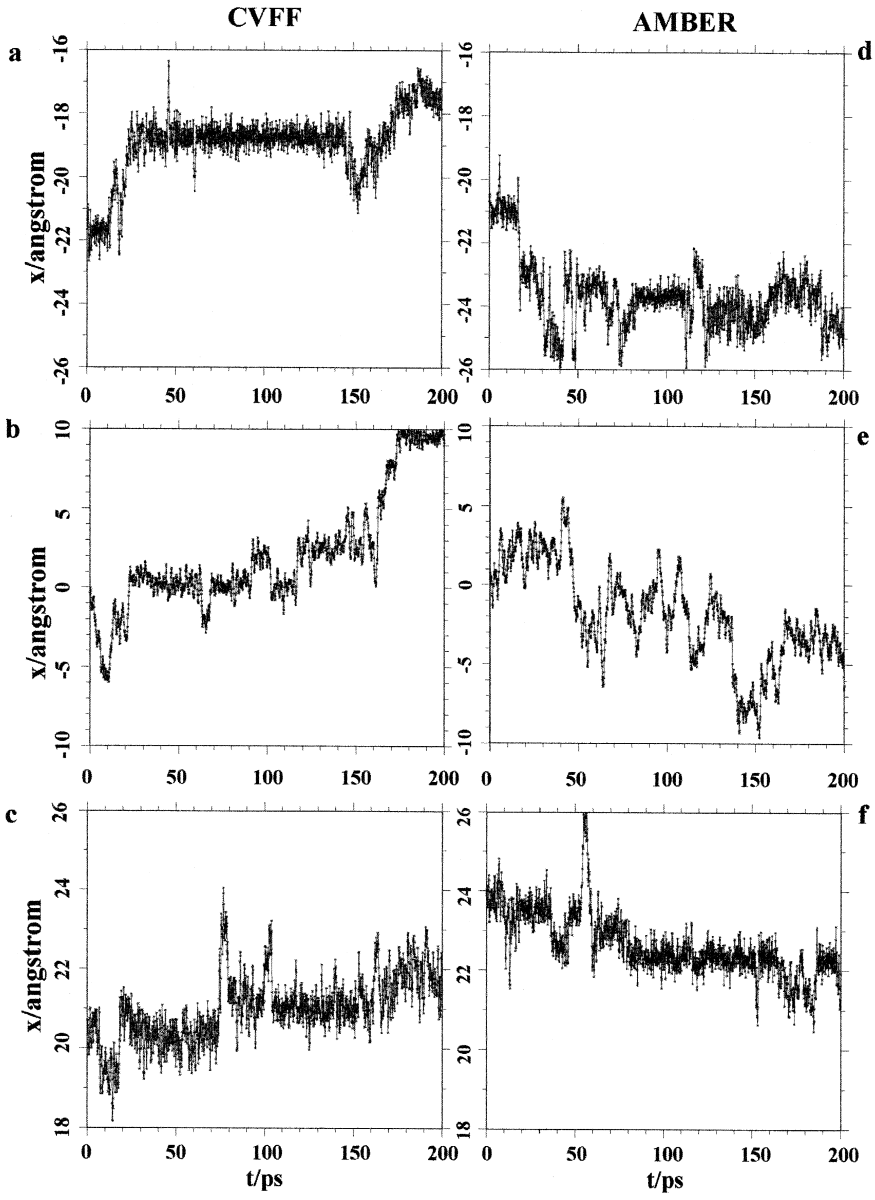

Fig. 4. Zoomed in trajectories from Fig. 3 for selected water molecules located at left (a and d), middle (b and e) and right (c and f) side of the pore. (a)–(c), from CVFF force field; (d)–(f), from AMBER force field.

that of the particles surrounding the intrapore water molecules. So the probability of collisions between water molecules and their surrounding particles is higher in the cap region than in the intrapore region.

Since water molecules wander through inhomogeneous regions with different diffusion constants (around 0.2–0.6 $Å^2/ps$ from rough estimation in our simulations) during translocation through the pore, this makes it difficult to describe the diffusion process in a general way. A simple way to solve this problem is to compute local diffusion constants by considering the diffusion within short time intervals, as done by others [9,10,27]. However, to get correct diffusion coefficients both the number of events and

enough time are necessary. An easier way to demonstrate the properties of intrapore water molecules is to use their standard deviations (s.d.) with respect to mean x-coordinates of their mass centers, which is related to the mean free displacements of water molecules here. Fig. 5 shows s.d. profiles of x-coordinates and nonbonded energies as a function of their mean x-coordinates for the same 33 water molecules as in Fig. 3. The water molecules in the intrapore region have larger s.d. values of x-coordinates, while the cap water molecules have smaller values (see Fig. 5a). In contrast, s.d. values of energies do not have such characteristic distributions as shown in Fig. 5b. So there is no correlation between the motions of water molecules and their energy variations, indicating the random movements of individual water molecules (see discussion in Section 3.3). This result also showed that the mean free displacements of intrapore water molecules are larger than those of the cap water molecules. Thus, it is consistent well with the inference from trajectories of pore water molecules, suggesting that there are more collisions between the water molecule and its surrounding particles in the cap region than in the pore region.

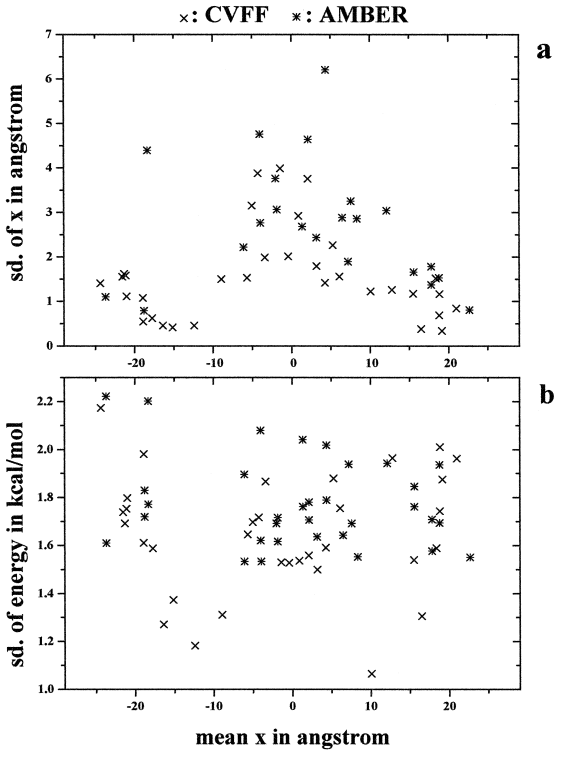

Fig. 5. Standard deviation profiles of x-coordinates (a) or nonbonded energy (b) as a function of mean x-coordinates for the same 33 water molecules as in Fig. 3. Data were from CVFF (×) or AMBER (∗) force field.

3.3. Dynamic energy profiles

In order to attain a more detailed description of the properties of intrapore water, we calculated the dynamic energy fluctuations of individual intrapore water molecules along the channel axis. The saved dynamic trajectories, which contain all the information about the dynamic properties of the system were replayed to calculate dynamic nonbonded interactions between each of 33 water molecules, which comes from the same source as in Fig. 3 and all of the rest of the atoms under 2000 conformations. As the channel was filled with water, the plot of interaction energies of each water molecule vs. its coordinate of mass center along the channel axis at a moment (corresponding to one of 2000 conformations) is corresponding to the energy profile at that moment. Combining the plots at all the moment together gives the dynamic energy profile. In this way, the behavior of water molecules at various positions in the channel were examined. A similar consideration was made previously [28,21], where energy profiles were calculated by fixing the ion at various positions along the channel axis and optimizing the configuration of the channel system. However, because their energy profiles are extracted from energy minimized configurations, an adiabatic energy profile does not account for thermal fluctuations and, thus, corresponds to a profile at 0 K [26].

The calculated dynamic energy profiles, which demonstrate the temporal and spatial variations of nonbonded interactions of individual water molecules, are shown in Fig. 6, in which rapid dynamic fluctuations of these interactions can be seen clearly. Although the energies fluctuate in a wide range, the coulombic interaction, contributed from all the rest of the atoms to the 33 selected water molecules always give negative values (see Fig. 6a and e), i.e., stabilizing these water molecules. The

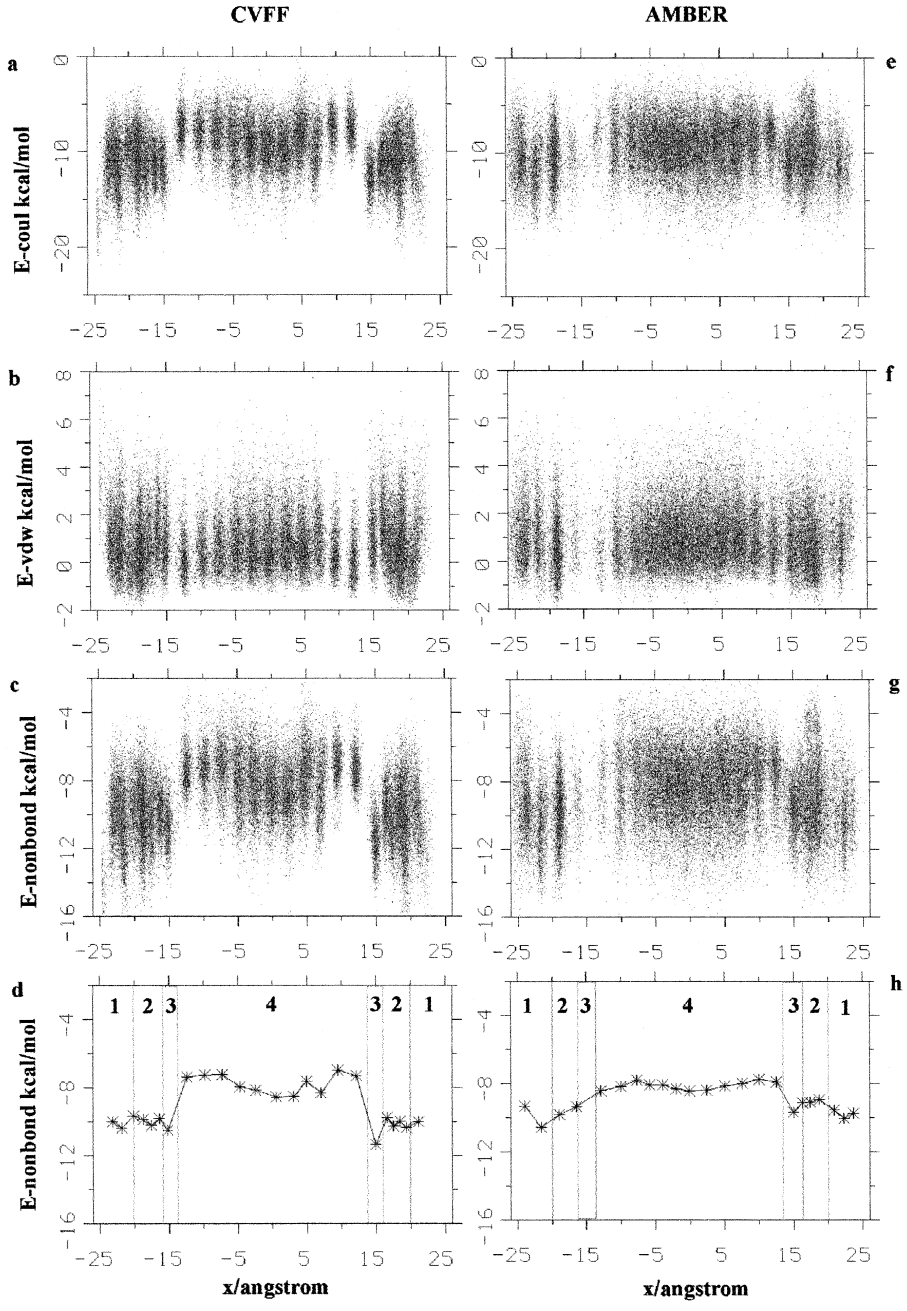

Fig. 6. Dynamic energy profiles of coulombic (a and e), van der Waals (b and f) and total nonbonded (c and g) interactions for water permeation through the channel. Data were obtained by calculating each corresponding interaction between a water molecule under study and all other atoms under 2000 conformations as a function of *x*-coordinate of mass center of the water molecule. Each datum is represented by a dot in the plot. (a)–(d), from CVFF force field; (e)–(h), from AMBER force field. (d) and (h) are the energy profiles for water permeation through the channel obtained by connecting mean energy values (∗) of each corresponding band in (c) and (g). Regions 1, 2, 3 and 4, which are divided by vertical lines, represent the cap water, the peptide ring, the junction and the middle region of the AC164 channel, respectively.

nonbonded energies of water molecules are generally lower in cap region than in middle region of the pore as illustrated in Fig. 6c, d and g, h. The energy barrier of the middle region of the pore relative to the energy level of the cap region for water to permeate through the pore was approximately 3.5 kcal/mol with CVFF force field and 2 kcal/mol with AMBER force field (Fig. 6d and h). These values are much less than ca. 8–10 kcal/mol of the ion permeation through gramicidin channel [26] and ca. 6 kcal/mol of water permeation through lipid bilayer membranes [27]. The dynamic energy level of the water molecule at the junction region, where the water molecules are surrounded by four carbonyl

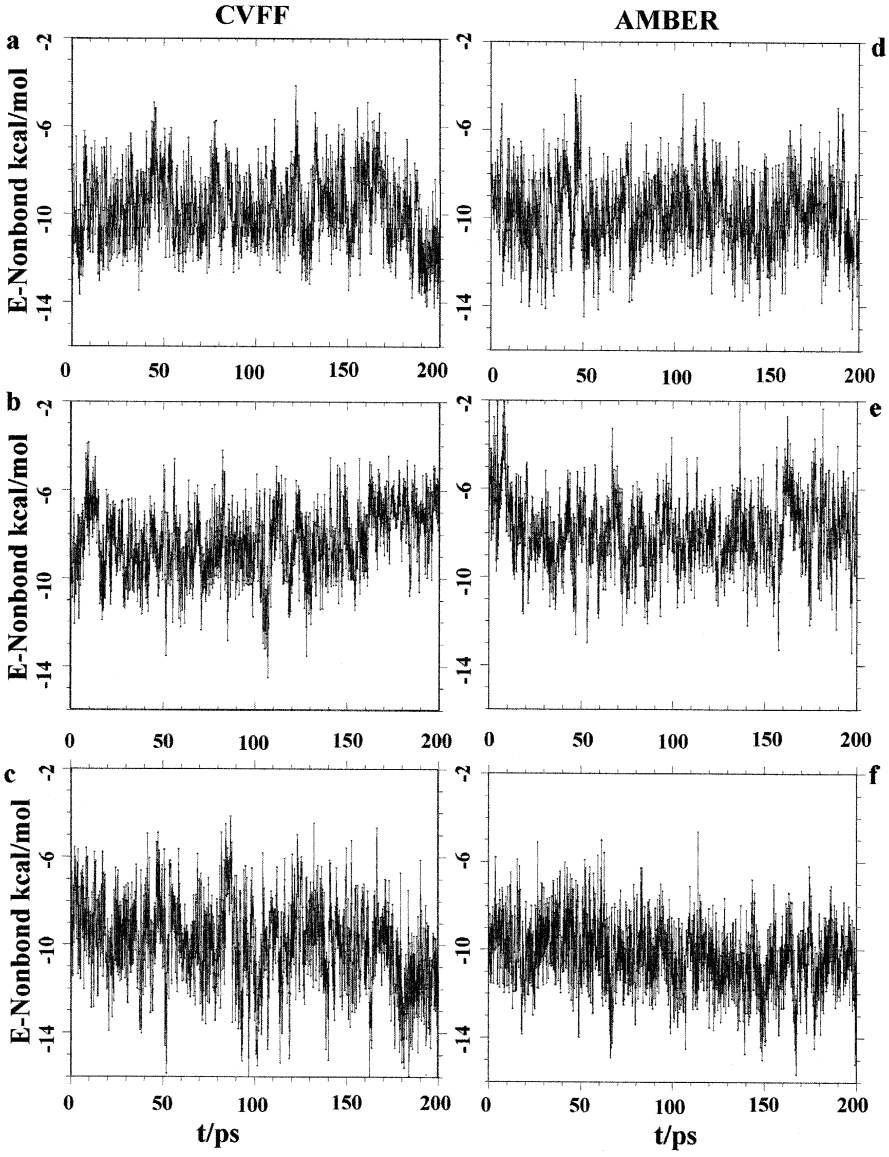

Fig. 7. Close view of dynamic energy fluctuations of the same water molecules in Fig. 4 as a function of time. Energy data were extracted from Fig. 6c and g.

oxygen atoms (indicated by large arrows in Fig. 1d and region 3 in Fig. 6d and h), was lower than the energy level of neighboring water molecules, suggesting that this region would behave as a 'binding site' for water. This is in accordance with our electrophysiological experiment, where it was suggested that the binding sites for monovalent cations to permeate through this channel are located near each entrance of the pore [11]. This was also implicated in Fig. 3 where the motion of the water molecule at the position of the 'binding sites' shown by large arrows is limited. Discrete bands in junction region (see Fig. 6c and g) are apparent, which means that water molecules prefer to stay some positions near the junction region. This phenomenon was clearly demonstrated in Fig. 3, when a water molecule jumped away from its current position another one promptly filled in.

It is noteworthy to mention here the fact that the energy profile obtained upon introducing all terms in the energy calculation is similar to that of the coulombic component alone (compare Fig. 6a,b and c or Fig. 6e,f and g), showing that the coulombic interaction predominates the interaction between water molecules and their surroundings even in a hydrophobic pore. The shape of mean energy profile roughly shown by the curves in Fig. 6d and h is in good agreement with the free energy profile of water transport through the lipid bilayer membrane [27], except for its lower barrier probably due to the relatively stable cavity created by the rigid ring structure of the AC164 molecule. The 'noise' level caused by thermal fluctuations can be reduced by making energy minimizations on the various generated conformations as was done in a previous study [25]. The problem of doing so is that the fully minimized conformations are associated with temperature approaching 0 K.

Fig. 7 shows fluctuations of nonbonded interaction energies as a function of time for the same water molecules as in Fig. 4. Comparing the trajectories of individual water molecules in Fig. 4 with variations of their nonbonded energy levels in Fig. 7, we found no correlation between the trajectory and energy variation. This means that the movement of each water molecule does not correlate with its energy level, implying that individual water molecules do not feel their energy levels.

3.4. Validity of the simulation results

As shown in Table 3, the thermodynamic quantities of the system are stable. This means that the whole system was in its equilibrium state during data collecting stage of the MD run. The demerit of using the extended wall region boundary condition (see Section 2.3) is that the fixed atoms in the middle and outer layers of water molecules and $-CH_2-$ particles might affect the relaxation of structure and density changes in the inner region where no atoms were fixed. To make such influence as small as possible, the conformation of the whole system was optimized before the MD run; the inner layer of water molecules and $-CH_2-$ particles are not emphasized in the simulation and can be taken as a buffer region to get information on the intrapore water. Thus, the influence of the fixed atoms on the intrapore water should have been reduced to the minimum.

In essence, force field is an empirical fit to the potential energy surface of molecules or functional groups. An important aspect of the force field is to set parameters satisfying proper energetic balance among their potential terms [19]. Therefore, in general, different results may be calculated from different force fields. In this sense, the common features of intrapore water obtained from the two independent simulations by using CVFF and AMBER force fields offer a strong test for the reliability of the results.

4. Conclusions

Dynamic properties of the water molecules in the AC164 hydrophobic channel were investigated using molecular dynamics simulations. Some common results were obtained from two independent MD runs with different force fields. These results suggested: (a) The water molecules could stably stay in the pore lined with hydrophobic acyl chains; (b) dynamic energy profiles with rapid energy fluctuations of individual water molecules were obtained, indicating that the mean energy barrier of water permeation through the pore is approximately 2–3 kcal/mol; (c) the internal diffusion of each water molecule is a process of a random walk and water molecules undergo more collisions in the cap region than in the pore region.

Acknowledgements

This work was supported in part by grants-in-aid for scientific research (to MS) from the Ministry of Education, Science and Culture of Japan.

References

[1] A. Parsegian, Nature 221 (1969) 844.
[2] P.C. Jordan, Biophys. J. 58 (1990) 1133.
[3] M. Sokabe, in: F. Oosawa, H. Hayashi, T. Yoshioka (Eds.), Transmembrane Signaling and Sensation, JSSP/VNU Science Press BV, Tokyo, 1984, p. 119.
[4] F. Hayashi, M. Sokabe, M. Takagi, K. Hayashi, U. Kishimoto, Biochim. Biophys. Acta 510 (1978) 305.
[5] M.J. Pregel, L. Jullien, J. Canceill, L. Lacombe, J.M. Lehn, J. Chem. Soc., Perkin Trans. 2 (1995) 417.
[6] Y. Tanaka, Y. Kobuke, M. Sokabe, Angew. Chem., Int. Ed. Engl. 34 (1995) 693.
[7] M. Sokabe, Z. Qi, K. Donowaki, H. Ishida, K. Okubo, Biophys. J. 70 (1996) A201.
[8] H. Ishida, K. Donowaki, Y. Inoue, Z. Qi, M. Sokabe, Chem. Lett. (1997) 953.
[9] M.S.P. Sansom, I.D. Kerr, J. Breed, R. Sankararamakrishnan, Biophys. J. 70 (1996) 693.
[10] J. Breed, R. Sankararamakrishnan, I.D. Kerr, M.S.P. Sansom, Biophys. J. 70 (1996) 1643.
[11] Z. Qi, M. Sokabe, Jpn. J. Physiol. 46 (1996) S99.
[12] M. Nilges, A.T. Brünger, Protein Eng. 4 (1991) 649.
[13] I.D. Kerr, R. Sankararamakrishnan, O.S. Smart, M.S.P. Sansom, Biophys. J. 67 (1994) 1501.
[14] Z. Qi, M. Sokabe, Biophys. J. 72 (1997) A399.
[15] E. Egberts, S.J. Marrink, H.J.C. Berendsen, Eur. Biophys. J. 22 (1994) 423.
[16] B. Roux, B. Prod'hom, M. Karplus, Biophys. J. 68 (1995) 876.
[17] P. Dauber-Osguthorpe, V.A. Robert, D.J. Osguthorpe, J. Wolff, M. Genest, A.T. Hagler, Proteins 4 (1988) 31.
[18] S.J. Weiner, P.A. Kollman, D.T. Nguyen, D.A. Case, J. Comp. Chem. 7 (1986) 230.
[19] W.F. van Gunsteren, A.E. Mark, Eur. J. Biochem. 204 (1992) 947.
[20] S. Nosé, Prog. Theor. Phys. 103 (1991) 1, Supplement.
[21] C. Etchebest, A. Pullman, FEBS. 204 (1986) 261.
[22] M.C. Wahl, M. Sundaralingam, TIBS. 22 (1997) 97.
[23] A. Skerra, J. Brickmann, Biophys. J. 51 (1987) 969.
[24] A. Skerra, J. Brickmann, Biophys. J. 51 (1987) 977.
[25] S.W. Chiu, S. Subramaniam, E. Jakobsson, J.A. McCammon, Biophys. J. 56 (1989) 253.
[26] B. Roux, M. Karplus, Annu. Rev. Biophys. Biomol. Struct. 23 (1994) 731.
[27] S.J. Marrink, H.J.C. Berendsen, J. Phys. Chem. 98 (1994) 4155.
[28] A. Pullman, C. Etchebest, FEBS. 163 (1983) 199.